

## Adhesion and peeling forces of carbon nanotubes on a substrate

Makoto Ishikawa,<sup>1</sup> Ryuichi Harada,<sup>2</sup> Naruo Sasaki,<sup>3</sup> and Kouji Miura<sup>1,2,\*</sup>

<sup>1</sup>*JST Plaza, Ahara-cho 23-1, Minami-ku, Nagoya 457-0063, Japan*

<sup>2</sup>*Department of Physics, Aichi University of Education, Kariya, Aichi 448-8542, Japan*

<sup>3</sup>*Department of Materials and Life Science, Faculty of Science and Technology, Seikei University, 3-3-1 Kichijoji-Kitamachi, Musashino-shi, Tokyo 180-8633, Japan*

(Received 25 February 2009; published 12 November 2009)

The adhesion and peeling of a multiwalled carbon nanotube (MWCNT) on a substrate have been studied. Nanoscale and mesoscale intermittent adhesion and peeling, and a conformational transition of an MWCNT appear in the vertical force-distance curve, which depends strongly on the length of the MWCNT, substrate, and velocities of adhesion and peeling. The elastic bending feature of the MWCNT as a nanospring appears during the adhesion and peeling.

DOI: [10.1103/PhysRevB.80.193406](https://doi.org/10.1103/PhysRevB.80.193406)

PACS number(s): 61.46.Np, 46.50.+a, 68.37.Ps, 81.40.Np

Detachment and peeling experiments are expected to provide information on adhesion forces and adhesion energies of solid surfaces in contact. Such experiments are important in powder technology, in the formation of adhesive films, and in understanding how cracks propagate in solid and how fracture occurs.<sup>1</sup> Recently, nanoscale peeling has been studied by extending biological polymer chains such as proteins using atomic force microscopy to clarify the mechanical mechanism of unfolding of the polymer chain. Such experiments have attracted much attention worldwide as a new method of spectroscopy for the structural analysis of biological macromolecules.<sup>2,3</sup> On the other hand, it has been more recently reported that carbon nanotube arrays with a curly entangled top show a macroscopic adhesive force of approximately 100 N per square centimeter, almost ten times that of a gecko foot and a shear adhesion force much stronger than the normal adhesion force.<sup>4</sup>

Therefore, we focused our attention on the elementary processes of adhesion and peeling of a nanotube on a substrate and have performed adhesion and peeling experiments using a multiwalled carbon nanotube (MWCNT). An MWCNT has been attached parallel to the cantilever to easily peel off the substrate to elucidate the elementary process of adhesion and peeling mechanisms.

We use a self-detecting cantilever (NPX1CTP003, SII) as a force sensor.<sup>5</sup> The system has a three-dimensional inertial-driven actuator (UNISOKU Co., Ltd.) as a sample stage. Thus, the base plate can be set on the conventional stage of a scanning electron microscope (SEM) (S-3000N, Hitachi, base pressure of  $2 \times 10^{-3}$  Pa), instead of the normal sample holder. The sample stage is controlled by a computer via an A/D, D/A compatible board. SEM images can be recorded as a movie using a video recorder. Because the resolution of A/D is 10 mV, the maximum resolution of the force sensor is approximately 0.1 nN. The fabrication of an MWCNT attached probe is performed in the SEM chamber. First, using the chemically etched metal probe that is fixed on the actuator, an MWCNT is pulled out from as-prepared MWCNT powder on the opposite support. Then, the MWCNT on the metal probe is moved toward the tip of a cantilever using an actuator. When an electron beam is irradiated around the contact junction between the MWCNT and the cantilever tip, the hydrocarbon is piled there and it works as glue. Finally, when the metal probe is quickly withdrawn, the MWCNT is

attached parallel to the cantilever. The handling of an MWCNT has been developed through improvements in the instruments described in previous reports.<sup>6,7</sup> Once the MWCNT has been sufficiently approached to the substrate surface using a coarse motion, the control was changed from coarse motion to fine motion. The adhesion and peeling experiments were repeated using fine motion.

Figure 1(a) shows the vertical force-distance curve using a 400-nm-long MWCNT, where the black and red lines represent adhesion and peeling, respectively. Several frames in the movie recorded during the adhesion and peeling are shown in Fig. 1(b), which are also visible in the movie.<sup>8</sup> Figure 1(c) shows the illustrations of the conformational configuration of the MWCNT during the peeling shown in Fig. 1(b). The white reversed triangle and white bar on the upper side and the horizon on bottom of each picture in Fig. 1(b) represent the tip of the cantilever, the MWCNT attached to the tip apex and the graphite surface, respectively. At first, the MWCNT takes an initial structure parallel to the graphite substrate surface. When the tip further approaches the graphite surface, the MWCNT attached to the tip apex comes into contact with the graphite surface [point A in Fig. 1(a)]. When the tip presses furthermore the graphite surface, the latter deforms downward with increasing repulsive force. When the peeling begins (red line), the vertical force  $F_z$  rapidly decreases while holding the line contact between the MWCNT and the graphite surface. As the MWCNT is peeled further from the graphite surface, the transition of the MWCNT shape occurs, which causes the first discontinuous jump ( $J_1$ ) in the  $F_z$  curve. Just after the discontinuous jump  $J_1$ , the point contact between the MWCNT and the graphite surface is formed. Frames D and E show the point contact formed between the free edge of the MWCNT and the graphite surface. Here the free edge is pushed onto the graphite surface and atoms on the free edge receive repulsive interaction forces.<sup>9-12</sup> As the MWCNT is peeled further, the free edge of the MWCNT slides on the graphite surface with increasing MWCNT bending in the period between  $J_1$  and  $J_2$ . The further retraction of the MWCNT from the surface decreases the repulsive force acting on atoms on the free edge and a relative increase in the effect of the attractive interaction force as shown in Fig. 1(a).<sup>9-12</sup> Now, when the bending of the MWCNT becomes larger than a certain range, the point contact breaks and the MWCNT is completely peeled

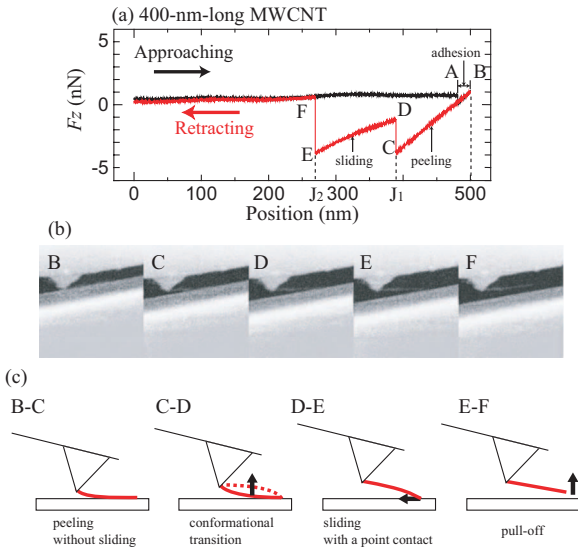


FIG. 1. (Color) (a) Vertical force-distance curve measured for the probe of a 400-nm-long MWCNT. (b) Several frames in the movie recorded during adhesion and peeling. (c) Schematic of (b).

from the surface, which makes the last discontinuous jump in the force curve ( $J_2$ ). When the second discontinuous jump ( $J_2$ ) occurs, the edge of the MWCNT is completely retracted from the graphite surface. Frames E and F show the images before and after the second discontinuous jump ( $J_2$ ), respectively. After the MWCNT is moved upward further, the MWCNT takes an original line shape parallel to the graphite surface because the effect of van der Waals interaction from the surface becomes negligibly small and  $F_z$  gradually becomes zero.

Figure 2 shows how the vertical force-distance curve depends on the length of the MWCNT. Figure 2(a) is the vertical force-distance curve obtained with the 400-nm-long MWCNT, which is the same as the curve shown in Fig. 2(b). Figures 2(b) and 2(c) show the vertical force-distance curves of the MWCNTs with lengths of 660 and 2380 nm, respectively. The black and red lines in each figure represent the force during the adhesion and peeling, respectively. In the approach shown in Fig. 2(b), small stick-slip behaviors appear at the region between B and C after the sudden line contact at A during the adhesion. Small stick-slip behaviors are also observed in the slope between C and D during the peeling, which exhibits a nanoscale intermittent adhesion and peeling without sliding. The discontinuous jump D-E in the peeling shown in Fig. 2(b) shows a conformational transition of the MWCNT. In the slope between E and F, a point contact between the MWCNT and the graphite surface is formed. For a 2380-nm-long MWCNT [Fig. 2(c)], the vertical force-distance curve becomes more complex and the number of discontinuous jumps increases, which exhibits a mesoscale intermittent peeling. Small stick-slip behaviors are also observed at the slopes, which exhibit a nanoscale intermittent peeling without sliding. At the discontinuous jump E-D, the MWCNT bends upward and performs a conformational transition. In the slope between E and F, the point contact between an MWCNT edge and graphite is formed with sliding.

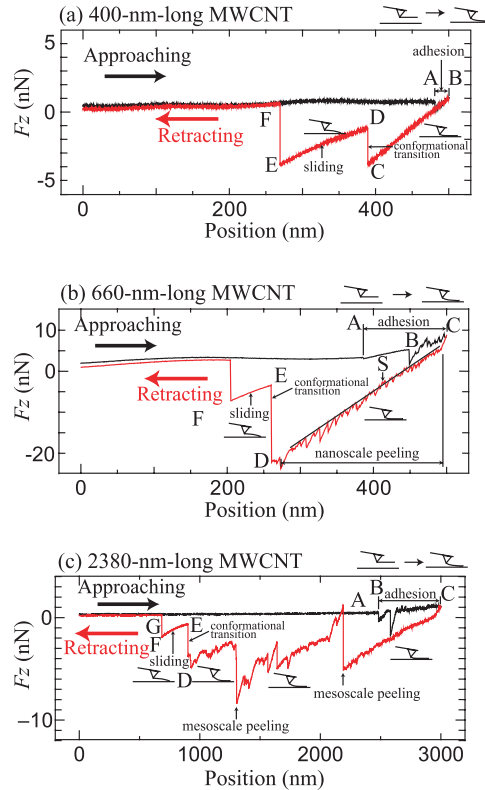


FIG. 2. (Color) Vertical force-distance curves measured using (a) 400-nm-long, (b) 660-nm-long, and (c) 2380-nm-long MWCNTs.

Here, it should be noted that both the mesoscale and nanoscale adhesions appear in the vertical force-distance curve during the adhesion. This feature resembles that of the force-distance curve during the peeling, which indicates that a part of the MWCNT comes into sudden line contact with the graphite surface during the approach. It is also revealed in this experiment that as the length of the MWCNT attached to the tip apex increases, the number of discontinuous jumps due to the mesoscale intermittent adhesion and peeling also increases; moreover, the nanoscale intermittent adhesion and peeling appear. This is because the long nanotube behaves like a soft spring, as shown in the simulation.<sup>9-12</sup> Namely, as the nanotube length increases, the contact time between a nanotube and a substrate during peeling also increases and thus, a large bending induces a large peeling. Interestingly, it is found that the elastic bending feature of the MWCNT as a nanospring appears in the vertical force-distance curve. Thus, the use of a much softer nanotube is expected to result in a much smaller intermittent adhesion and peeling than those of the nanoscale one.

Furthermore, effect of the peeling velocity on the peeling force is investigated. In the force-distance measurement, the external force  $f$  is added to the MWCNT to peel it off the substrate. Thus, the energy barrier height for bonds formed between the MWCNT and substrate is lowered by  $fx_\beta$  with the external force  $f$ , where  $x_\beta$  means the effective distance of the potential barrier from the minimum point needed to break the bond, as illustrated in Fig. 3(k). Then the lifetime for bond is expressed as follows:<sup>2,3</sup>

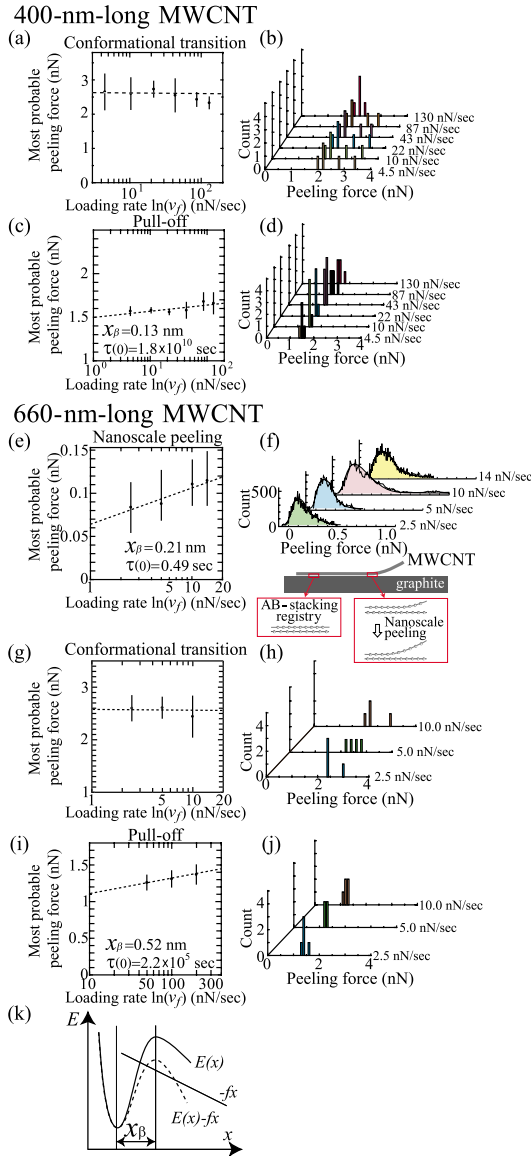


FIG. 3. (Color online) The histogram of the peeling force and the most probable peeling force  $f^*$  at various force loading rate,  $v_f$  for all the processes of the nanoscale peeling, conformational transition, and pull off for 400-nm-long MWCNT and 660-nm-long MWCNT. Conceptual energy landscapes  $E$  for bonds are illustrated in (k). The energy barrier height for bonds formed between the MWCNT and substrate is lowered by  $fx_\beta$  with the external force  $f$ .

$$\tau(f) = \tau(0)\exp(-fx_\beta/k_B T), \quad (1)$$

where  $k_B$ ,  $T$ , and  $\tau(0)$  mean the Boltzmann constant, the temperature, and the natural lifetime, respectively. If the external force  $f$  is applied with a constant loading rate  $v_f$  as a function of time  $t$  in the force-distance measurement, then  $f(t) = v_f t$ . Since the lifetime  $\tau(f)$  is the inverse of the rate of dissociation, the probability of the existing bonds,  $S$  is given as follows:

$$dS/dt = -S/\tau(f). \quad (2)$$

$S(t)$  is given as follows using  $S(0) = 1$ ,

$$S(t) = \exp\left[-\int_0^t \frac{1}{\tau(f)} dt\right]. \quad (3)$$

The probability  $P(f)$  that the bond breaks if the external force  $f$  acts on it is given by  $-dS/df$ ,

$$P(f) = \frac{\exp\left[-\int_0^t \frac{1}{\tau(f)} dt\right]}{v_f \tau(f)}. \quad (4)$$

If  $dP/df = 0$ , the most probable peeling force  $f^*$  is given as follows by Evans *et al.*,<sup>2</sup>

$$f^* = \frac{k_B T}{x_\beta} \ln(v_f) + \frac{k_B T}{x_\beta} \ln\left[\frac{\tau(0) \cdot x_\beta}{k_B T}\right]. \quad (5)$$

Now the peeling velocities are set as 10–1000 nm/s. The nanoscale intermittent behaviors for the MWCNTs with lengths of 660 and 2380 nm, depend strongly on the peeling velocities as shown in Fig. 3(e). Since the peeling is a stochastic process, it is possible that the most probable nanoscale intermittent peeling force,  $f^*$ , is given as a function of the loading rate,  $v_f$ , obtained from the peak of the histogram of the peeling force  $f^*$  specified by the Gaussian distribution,<sup>2,3</sup> which is taken from peak heights from the straight line [see the line S in Fig. 2(b)] keeping a constant loading rate. Since it is clearly shown that  $f^*$  is linearly related to the logarithm of the loading rate,  $v_f$ , the obtained  $v_f f^*$  relation can be fitted to the logarithmic relation of Eq. (5) obtained by Evans *et al.*<sup>2</sup>  $x_\beta$  and  $\tau(0)$  have been estimated to be 0.21 nm and 0.49 s from the slope and the  $x$  intersection of the fitting line as shown in Fig. 3(e), respectively. The order of magnitude of the position of the potential barrier,  $x_\beta$ , is comparable to that of the atomic-scale distance between the neighboring stable *AB*-stacking positions within  $x$ - $y$  plane. Here the *AB*-stacking registry formed between a graphite flake and a graphite substrate surface is considered.<sup>13,14</sup> This indicates that the peeling of the MWCNT starts when the outermost graphene sheet of the MWCNT goes over the potential barrier of the *AB*-stacking registry with the graphite substrate surface, as depicted in the lower part of Fig. 3(f). Thus the nanoscale intermittent behaviors occur due to the atomic-scale stochastic sliding of the MWCNT activated thermally within the  $x$ - $y$  plane on the graphite substrate, which appears in the vertical force curve as shown in Figs. 2(b) and 2(c).

However, it was found that the pull-off forces in the vertical force-distance curve in all the MWCNTs depend weakly on the peeling velocities. Figure 3(c) shows  $x_\beta = 0.13$  nm and  $\tau(0) = 1.8 \times 10^{10}$  s for the 400-nm-long MWCNT. Similarly Fig. 3(i) exhibits  $x_\beta = 0.52$  nm and  $\tau(0) = 2.2 \times 10^5$  s for the 660-nm-long MWCNT. This indicates that the shorter MWCNT requires a larger force to pull off the graphite substrate than the longer MWCNT. In either case, it is difficult to pull MWCNTs off the graphite substrate without a lifting force because a natural lifetime  $\tau(0)$  is infinitely large. On the other hand, the mesoscale intermittent forces of the conformational transition for 400-nm-long MWCNT, 660-nm-long MWCNT, and 2380-nm-long MWCNT are almost constant [Figs. 3(a) and 3(g)] or slightly decrease with an

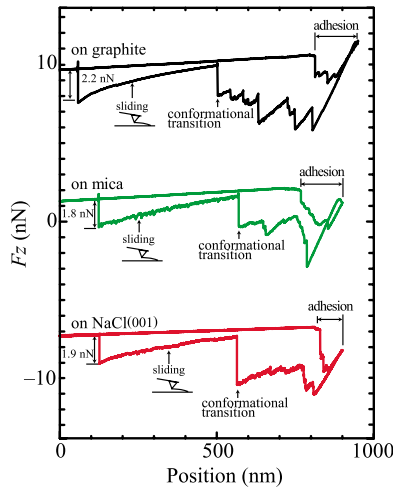


FIG. 4. (Color online) Vertical force-distance curves measured on graphite, mica, and NaCl(001) surfaces.

increase in the loading rate, which indicates that the barrier position  $x_\beta$  of the conformational transition is at least on the order of a MWCNT length and then the slope  $k_B T/x_\beta$  in Eq. (5) nearly goes to zero. Here it should be also noted that the conformational transition occurs within the  $x$ - $z$  plane.

To investigate the effect of substrate on the adhesion and peeling behaviors of an MWCNT, the vertical force-distance curve was measured for graphite, mica, and NaCl(001) surfaces, as shown in Fig. 4. First, it was found that the pull-off forces of an MWCNT edge on the substrate corresponding to the final jumps are 2.2, 1.8, and 1.9 nN for graphite, mica, and NaCl(001), respectively, which shows that the interaction strength between an MWCNT edge and a substrate is strongest for the graphite surface and comparable for the mica and NaCl(001) surfaces. In the vertical force-distance curve of the graphite surface, the number of discontinuous jumps corresponding to the mesoscale intermittent peeling increases, which is not observed for the mica and NaCl(001) surfaces. This is because, as the interaction strength between the MWCNT and the substrate surface increases, the contact time between them during the peeling becomes longer and thus, a large bending induces a large peeling. It is thus interesting to note that the features of the vertical force-distance curve in case of the strong interaction between an MWCNT and a substrate resemble those in the case of the soft MWCNT.

Furthermore, to investigate the effect of adsorbates on the

adhesion and peeling mechanisms, we have performed experiments on the vertical force-distance curve under ambient conditions. The vertical force-distance curve with the characteristic hysteresis loop obtained under ambient conditions was almost the same as that obtained using an SEM, which indicates that humidity and ambient gases do not strongly affect the main feature of the vertical force-distance curve.

In this work, adhesion and peeling experiments on the MWCNT have been performed. We have experimentally obtained the vertical force-distance curve with the characteristic hysteresis loop, which exhibits multistable states between line contact and point contact of the MWCNT shape during the adhesion and peeling. The line and point contacts are clearly divided by the discrete jump that appeared in the vertical force-distance curve, which shows the nanoscale elastic property of the MWCNT. The adhesion and peeling behaviors of the MWCNT reveal hierarchical structures (or fractal structures) from the nanoscale intermittent to the mesoscale intermittent adhesion and peeling. The nanoscale intermittent behaviors depend strongly on the adhesion and peeling velocities, which reveals that the peeling occurs when a MWCNT goes over the potential barrier of the neighboring *AB*-stacking registry with the graphite substrate surface. On the other hand, the most probable pull-off forces depend weakly on the peeling velocities, which indicate that it is difficult to pull MWCNTs off the graphite substrate without a finite lifting force. Furthermore the mesoscale intermittent forces of the conformational transition indicate that the barrier position of the conformational transition is at least on the order of a MWCNT length.

This technique will be applicable not only to material science but also to molecular biology because this system makes it possible to analyze the physical properties of a cell, protein molecules, and DNA. These results could also provide information on the mechanisms of how to make an adhesion and how a gecko performs, and could be used to propose a guiding principle for designing the artificial superadhesive system beyond a gecko foot. The detailed discussions based on more general theoretical approach of the multiscale peeling will be performed in the near future.

This research was supported by a Grant-in-Aid for Scientific Research from the Japan Society for the Promotion of Science (Grants No. 16340089, No. 18340087, and No. 20360022) and “Practical Application Research, Science and Technology Incubation Program in Advanced Regions,” Japan Science and Technology Agency.

\*Corresponding author; kmiura@aeucc.aichi-edu.ac.jp

<sup>1</sup>J. N. Israelachvili, *Intermolecular and Surface Forces* (Academic, London, 1992).

<sup>2</sup>E. Evans *et al.*, *Biophys. J.* **59**, 838 (1991).

<sup>3</sup>M. Rief *et al.*, *Science* **275**, 1295 (1997).

<sup>4</sup>L. Qu *et al.*, *Science* **322**, 238 (2008).

<sup>5</sup>M. Ishikawa *et al.*, *Appl. Phys. Lett.* **93**, 083122 (2008).

<sup>6</sup>M. Ishikawa *et al.*, *Physica B* **323**, 184 (2002).

<sup>7</sup>M. Ishikawa *et al.*, *Appl. Surf. Sci.* **188**, 456 (2002).

<sup>8</sup>For movies, visit <http://miuralab.com/box/movie/movie.html>

<sup>9</sup>N. Sasaki *et al.*, *e-J. Surf. Sci. Nanotechnol.* **4**, 133 (2006).

<sup>10</sup>N. Sasaki *et al.*, *e-J. Surf. Sci. Nanotechnol.* **6**, 72 (2008).

<sup>11</sup>N. Sasaki *et al.*, *e-J. Surf. Sci. Nanotechnol.* **7**, 48 (2009).

<sup>12</sup>N. Sasaki *et al.*, *e-J. Surf. Sci. Nanotechnol.* **7**, 783 (2009).

<sup>13</sup>K. Miura *et al.*, *Phys. Rev. Lett.* **90**, 055509 (2003).

<sup>14</sup>K. Miura *et al.*, *Phys. Rev. B* **69**, 075420 (2004).